Dynamics of a Mobile Robot with Three Ball-Wheels

February 17, 1999

Svetlana Ostrovskaya, Raymond J. Spiteri, Jorge Angeles
Department of Mechanical Engineering & Centre for Intelligent Machines,
McGill University, 817 Sherbrooke St. W., Montreal, Quebec,
Canada H3A 2K6
svetlana@cim.mcgill.ca spiteri@cim.mcgill.ca angeles@cim.mcgill.ca

Abstract

A mathematical model is developed for a mobile robot with three ball-wheels. The resulting model turns out to be a Chaplygin system, which allows the dynamic equations and the kinematic constraints to be integrated separately. The system is driven by six actuators: one actuator connected to one roller of each wheel, and three more actuators controlling the orientation of the ball-carriers with respect to the platform. Analysis of the mathematical model of this system using the *holonomy matrix* yields conditions under which the system can be rendered holonomic. Holonomy can be achieved by keeping the ball-carriers in pure translational motion. Therefore, the control of the system can be simplified by imposing constraints on the ball-carriers that prevent them from changing their orientation with respect to an inertial frame.

1 Introduction

Wheeled mobile robots (WMR) belong to a class of mechanical systems characterized by kinematic constraints that are *nonholonomic*. This implies that the generalized coordinates, which correspond to the so-called *dependent generalized velocities*, cannot be eliminated from the governing equations due to the constraints. As a result, nonholonomic mechanical models are highly complex from the computational standpoint, making their real-time control quite challenging. Moreover, nonholonomic constraints cause complexities in trajectory planning and in the design of control algorithms. As a consequence, standard planning and control algorithms developed for robotic manipulators are not applicable to WMR.

In approaching the problem of WMR, mechanisms for omnidirectional and holonomic wheeled mobile robots have been developed: the offset steered driving wheels [[17]], [[18]]; omnidirectional wheels [[6]], [[7]], [[13]]; spherical wheels (orthogonal wheels [[12]], [[16]]; ball-wheel omnidirectional mechanisms [[19]]; [[3]], [[20]], [[21]], [[22]]; [[5]]; [[11]]; [[4]], orthogonal-wheel assembly mechanisms [[12]], [[16]]; spherical robots [[1]]; etc.).

In this paper, a novel approach is introduced to the design of omnidirectional and holonomic wheeled vehicles, whereby a new mechanism is proposed. This mechanism, described in Section 2, consists of a platform with three identical ball-wheels constrained by three rollers each, with their respective axes fixed to ball-carriers. The geometric and kinematic constraints are derived and the holonomy matrix for these kinematic constraints is obtained. In Section 3, we derive the kinetic energy of this mechanical system, and we use it in Section 4 to develop the mathematical model of the system. We show that the model can be simplified by implementing the additional constraints to restrict the motion of the ball-carriers to pure translation. Finally, in Section 5, we include results of some numerical simulations.

2
Constraints and Generalized Coordinates

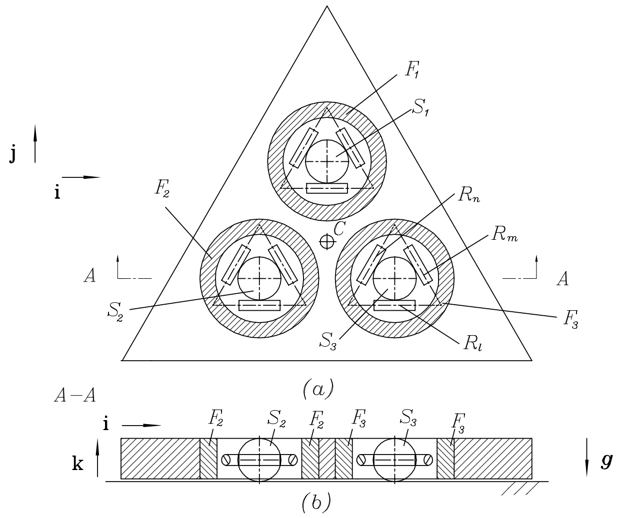

Figure 1: Rolling robot with three ball-wheels: (a) top view; (b) cross section AA.

A rolling robot with three ball-wheels is shown in Fig. 1. This robot consists of a triangular platform and three identical ball-wheels, S_1, S_2, and S_3. Each ball is constrained by three rollers that lie around the horizontal great circle of the ball, the roller axes forming an equilateral triangle;

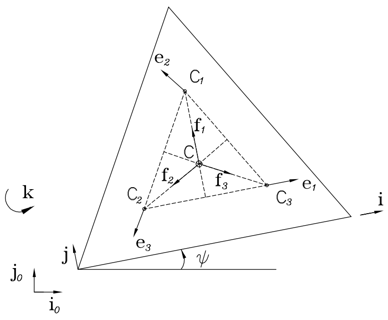

Figure 2: Definition of unit vectors.

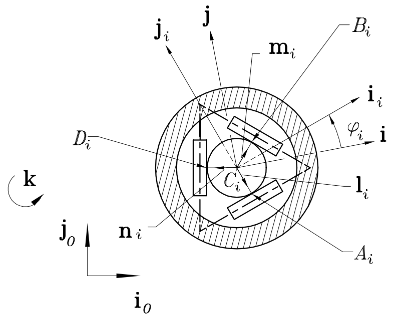

Figure 3: A ball-wheel.

these rollers are indicated as R_l, R_m, and R_n in Fig. 1a. Moreover, the axes of the rollers are fixed to ball-carriers F_i, for $i = 1, 2, 3$, that rotate with respect to the platform about vertical axes through the ball centers.

Let us define an orthonormal triad $\{\mathbf{i}_0, \mathbf{j}_0, \mathbf{k}\}$, which defines, in turn, an inertial frame, with $\mathbf{k}$ pointing in the upward vertical direction. Likewise, we define an orthonormal triad $\{\mathbf{i}, \mathbf{j}, \mathbf{k}\}$ that rotates with the platform of the robot, as shown in Fig. 2, and the triad $\{\mathbf{i}_i, \mathbf{j}_i, \mathbf{k}\}$ that rotates with the ith ball-carrier, as displayed in Fig. 3. The triad $\{\mathbf{i}_i, \mathbf{j}_i, \mathbf{k}\}$ rotates with respect to the triad $\{\mathbf{i}, \mathbf{j}, \mathbf{k}\}$ about a vertical axis with angular velocity $\dot{\varphi}_i$, while the triad $\{\mathbf{i}, \mathbf{j}, \mathbf{k}\}$ rotates with respect to the inertial frame $\{\mathbf{i}_0, \mathbf{j}_0, \mathbf{k}\}$ about a vertical axis with angular velocity $\dot{\psi}$. The position and orientation of all the bodies of the system can thus be described by 24 variables, namely, three for the platform position and orientation, $\mathbf{c}$, ψ, three angles representing the orientation of the ball-carriers with respect to the platform, $\{\varphi_i\}_1^3$, $3 \times 3 = 9$ angles representing the rotation of the rollers about their own axes, $\{\theta_{li}, \theta_{mi}, \theta_{ni}\}_{i=1}^3$, and $3 \times 3 = 9$ ball-wheel orientation variables.

Denoting by $\mathbf{c}_i$ the position vector of the mass center of the ith ball (Fig. 2), we have the relation

$$\mathbf{c}_i = \mathbf{c} + \mathbf{f}_i d \tag{1}$$

where d is the common horizontal distance between the mass center of the platform and that of the ball-carriers F_i, $\mathbf{e}_i$, and $\mathbf{f}_i$ being additional unit vectors that rotate with the platform as shown in Fig. 2. Upon differentiation of both sides of eqs.(1), we obtain

$$\dot{\mathbf{c}}_i = \dot{\mathbf{c}} - \dot{\psi}\mathbf{e}_i d. \tag{2}$$

Assuming that there is no slippage between the rollers and the balls, the system has 12 positional degrees of freedom (dof), and we can thus describe the configuration of the system by the 12-dimensional vector $\mathbf{q}$ of generalized coordinates

$$\mathbf{q} \equiv [\begin{array}{cccc} \psi & \mathbf{c}^T & \boldsymbol{\xi}^T & \boldsymbol{\varphi}^T \end{array}]^T \tag{3}$$

where ψ is the angle of rotation of the platform with respect to the inertial frame $\{\mathbf{i}_0,\ \mathbf{j}_0,\ \mathbf{k}\}$ and $\mathbf{c} = x\mathbf{i}_0 + y\mathbf{j}_0$ is the 2-dimensional position vector of the platform mass center represented in the inertial frame. Moreover, $\boldsymbol{\xi}$ is a 6-dimensional vector

$$\boldsymbol{\xi} \equiv \left[\begin{array}{ccc} \boldsymbol{\xi}_1^T & \boldsymbol{\xi}_2^T & \boldsymbol{\xi}_3^T \end{array} \right]^T , \tag{4}$$

whose definition is described below. Moreover, from the no-slip condition between the rollers and the ball, we derive the relations

$$\dot{\theta}_{li} + \dot{\theta}_{mi} + \dot{\theta}_{ni} = 0 \ . \tag{5}$$

Since each ball-wheel of this system has two dof, only two of the three angles $\{\theta_{li}, \theta_{mi}, \theta_{ni}\}$ are independent. Hence, we have only three possible choices (three ways to choose two out of three) to assign independent rotations to each wheel, namely, lm, mn, or nl. Therefore, we can express $\boldsymbol{\xi}_i$ as

$$\boldsymbol{\xi}_i \equiv \mathbf{K}\boldsymbol{\theta}_i \ , \quad i = 1, 2, 3 \quad \text{where} \quad \boldsymbol{\theta}_i \equiv \left[\begin{array}{ccc} \theta_{li} & \theta_{mi} & \theta_{ni} \end{array} \right]^T \tag{6}$$

and $\mathbf{K}$ is a 2×3 *selection matrix* that denotes the choice of two independent components of vector $\boldsymbol{\theta}_i$, i.e.,

$$\mathbf{K} \equiv \left[\begin{array}{ccc} 1 & 0 & 0 \\ 0 & 1 & 0 \end{array} \right], \text{ or } \mathbf{K} \equiv \left[\begin{array}{ccc} 0 & 1 & 0 \\ 0 & 0 & 1 \end{array} \right], \text{ or } \mathbf{K} \equiv \left[\begin{array}{ccc} 1 & 0 & 0 \\ 0 & 0 & 1 \end{array} \right]. \tag{7}$$

Finally, $\boldsymbol{\varphi}$ is the vector of ball-carrier orientations with respect to the platform, i.e., $\boldsymbol{\varphi} \equiv \left[\begin{array}{ccc} \varphi_1 & \varphi_2 & \varphi_3 \end{array} \right]^T$.

Further, assuming that there is no slippage between the wheels and the ground, we can derive the relation [[9]]

$$\dot{\mathbf{c}} - \dot{\psi}\mathbf{e}_i d - \boldsymbol{\omega}_i \times R\mathbf{k} = \mathbf{0}, \quad i = 1, 2, 3 \tag{8}$$

where $\boldsymbol{\omega}_i$ is the angular-velocity vector of ith ball-wheel, i.e., $\boldsymbol{\omega}_i = u_i\mathbf{i}_0 + v_i\mathbf{j}_0 + w_i\mathbf{k}_0$, and R denotes the radius of the ball-wheel.
Hence, for this system with 12 positional dof, we have six kinematic constraints. Therefore, the system has $12 - 6 = 6$ independent velocities, i.e. the *velocity degree of freedom*, or *mobility*, of the system is 6. Now we note that

$$\boldsymbol{\omega}_i \times \mathbf{k} = \left[\begin{array}{ccc} u_i & -v_i & 0 \end{array} \right]^T ,$$

and define the 2×2 matrix $\mathbf{E}$ and the two-dimensional vector $\mathbf{w}_i$ as

$$\mathbf{E} \equiv \left[\begin{array}{cc} 0 & -1 \\ 1 & 0 \end{array} \right] , \quad \mathbf{w}_i \equiv \left[\begin{array}{c} u_i \\ v_i \end{array} \right] . \tag{9}$$

We can thus rewrite the two independent scalar equations of eq.(8) in two-dimensional form as

$$\dot{\mathbf{c}} - \dot{\psi}\mathbf{e}_i d + R\mathbf{E}\mathbf{w}_i = \mathbf{0} \ . \tag{10}$$

The first two components u_i, v_i of the angular velocity vector of the ith ball can be derived in the form

$$\mathbf{w}_i = \rho\mathbf{R}_i^{-1}\dot{\boldsymbol{\xi}}_i$$

where $\mathbf{R}_i$ is defined as

$$\mathbf{R}_i \equiv \mathbf{K} \begin{bmatrix} -c_{li} & -s_{li} \\ -c_{mi} & -s_{mi} \\ -c_{ni} & -s_{ni} \end{bmatrix} \quad \text{and} \quad \rho \equiv \frac{r}{R}\,, \tag{11}$$

where we have introduced the notation

$$s_{ji} \equiv \sin(\psi + \varphi_i + \delta_j), \quad c_{ji} \equiv \cos(\psi + \varphi_i + \delta_j),$$

with $j = l, m, n$, for $i = 1, 2, 3$, and $\delta_l \equiv 0$, $\delta_m \equiv (2/3)\pi$, $\delta_n \equiv (4/3)\pi$. Substituting this expression into eq.(10), we obtain the constraint equation in the form:

$$\dot{\mathbf{c}} - \dot{\psi}\mathbf{e}_i d + r\mathbf{E}\mathbf{R}_i^{-1}\dot{\boldsymbol{\xi}}_i = \mathbf{0}. \tag{12}$$

If we choose the independent velocity vector $\mathbf{u}$ as $\mathbf{u} \equiv [\ \dot{\psi} \quad \dot{\mathbf{c}}^T \quad \dot{\boldsymbol{\varphi}}^T\ ]^T$ then, from eq.(12), we have

$$\dot{\boldsymbol{\xi}}_i = \boldsymbol{\Upsilon}_i \mathbf{u} \tag{13}$$

where $\boldsymbol{\Upsilon}_i$ is the 2×6 matrix given by

$$\boldsymbol{\Upsilon}_i \equiv \frac{1}{r}\left[\ \boldsymbol{\alpha}_i d \quad -\mathbf{S}_i \quad \mathbf{O}_{2\times 3}\ \right], \quad \boldsymbol{\alpha}_i \equiv \mathbf{R}_i\mathbf{E}^T\mathbf{e}_i, \quad \mathbf{S}_i \equiv \mathbf{R}_i\mathbf{E}^T, \tag{14}$$

and $\mathbf{O}_{i\times j}$ defined as the $i \times j$ zero matrix. Therefore, using definition (4), we can write

$$\dot{\boldsymbol{\xi}} = \boldsymbol{\Upsilon}\mathbf{u}, \quad \boldsymbol{\Upsilon} \equiv \left[\ \boldsymbol{\Upsilon}_1 \quad \boldsymbol{\Upsilon}_2 \quad \boldsymbol{\Upsilon}_3\ \right]^T. \tag{15}$$

Now we can express all generalized velocities in terms of the six independent velocities in the form

$$\dot{\mathbf{q}} = \mathbf{N}\mathbf{u}$$

with $\mathbf{N}$ being a 12×6 matrix

$$\mathbf{N} \equiv \begin{bmatrix} 1 & \mathbf{0}_2^T & \mathbf{0}_3^T \\ \mathbf{0}_2 & \mathbf{1}_{2\times 2} & \mathbf{O}_{2\times 3} \\ (d/r)\boldsymbol{\alpha} & -(1/r)\mathbf{S} & \mathbf{O}_{6\times 3} \\ \mathbf{0}_3 & \mathbf{O}_{3\times 2} & \mathbf{1}_{3\times 3} \end{bmatrix},$$

$\mathbf{0}_k$ denoting the k-dimensional zero vector and $\mathbf{1}_{i\times i}$ denoting the $i \times i$ identity matrix, while $\mathbf{q}$ is defined in (3) and

$$\boldsymbol{\alpha} \equiv \begin{bmatrix} \boldsymbol{\alpha}_1 \\ \boldsymbol{\alpha}_2 \\ \boldsymbol{\alpha}_3 \end{bmatrix}, \quad \mathbf{S} \equiv \begin{bmatrix} \mathbf{S}_1 \\ \mathbf{S}_2 \\ \mathbf{S}_3 \end{bmatrix}. \tag{16}$$

Furthermore, from eqs.(11), (9), and (14) we have, for $i = 1, 2, 3$,

$$\boldsymbol{\alpha}_i = \mathbf{K} \begin{bmatrix} \sin(\varphi_i + \delta_l - \delta_i) \\ \sin(\varphi_i + \delta_m - \delta_i) \\ \sin(\varphi_i + \delta_n - \delta_i) \end{bmatrix}, \quad \mathbf{S}_i = \mathbf{K} \begin{bmatrix} s_{li} & -c_{li} \\ s_{mi} & -c_{mi} \\ s_{ni} & -c_{ni} \end{bmatrix}. \tag{17}$$

The Holonomy Matrix

To test the holonomy of the system with the kinematic constraints of eqs.(12), we use the holonomy matrix

$$\mathbf{H} = \left[\frac{\partial(\mathbf{N}\mathbf{u})}{\partial\mathbf{q}}\mathbf{N} - \dot{\mathbf{N}}\right]^T , \tag{18}$$

introduced in [[9]]. The vanishing of this matrix is a necessary and sufficient condition for the system to be holonomic.

The holonomy matrix for this system has the form

$$\mathbf{H} \equiv \left[\frac{\partial(\mathbf{N}\mathbf{u})}{\partial\mathbf{q}}\mathbf{N} - \dot{\mathbf{N}}\right]^T = \frac{1}{r}\begin{bmatrix} \mathbf{0}_3^T & \mathbf{g}_1^T & \mathbf{g}_2^T & \mathbf{g}_3^T & \mathbf{0}_3^T \\ \mathbf{O}_{2\times 3} & \dot{\mathbf{S}}_1^T & \dot{\mathbf{S}}_2^T & \dot{\mathbf{S}}_3^T & \mathbf{O}_{2\times 3} \\ \mathbf{0}_3^T & \mathbf{b}_1^T & \mathbf{0}_2^T & \mathbf{0}_2^T & \mathbf{0}_3^T \\ \mathbf{0}_3^T & \mathbf{0}_2^T & \mathbf{b}_2^T & \mathbf{0}_2^T & \mathbf{0}_3^T \\ \mathbf{0}_3^T & \mathbf{0}_2^T & \mathbf{0}_2^T & \mathbf{b}_3^T & \mathbf{0}_3^T \end{bmatrix} \tag{19}$$

where, for $i = 1, 2, 3$,

$$\mathbf{a}_i \equiv -\frac{\partial\mathbf{S}_i}{\partial\psi}\dot{\mathbf{c}} = -\mathbf{S}_i'\dot{\mathbf{c}} ,$$

$$\mathbf{b}_i \equiv \frac{\partial\boldsymbol{\alpha}_i}{\partial\varphi_i}\dot{\psi}d - \frac{\partial\mathbf{S}_i}{\partial\varphi_i}\dot{\mathbf{c}} = \boldsymbol{\alpha}_i'\dot{\psi}d - \mathbf{S}_i'\dot{\mathbf{c}} = \boldsymbol{\alpha}_i'\dot{\psi}d + \mathbf{a}_i ,$$

and $\mathbf{g}_i \equiv \mathbf{a}_i - \dot{\boldsymbol{\alpha}}_i d$.

Thus, the holonomy matrix does not identically vanish; hence, the constraint equations (12) are nonintegrable and the system is nonholonomic. In Section 5, we study the conditions under which the system at hand can be rendered holonomic. In order to set up the mathematical model of the system using Lagrange's equations, we need an expression for its kinetic energy. This is now derived in Section 3.

3
The Kinetic Energy of the System

The twists of the platform and the ball-carriers can be expressed as the 3-dimensional vectors

$$\mathbf{t}_p = \begin{bmatrix} \omega_p \\ \dot{\mathbf{c}} \end{bmatrix} , \quad \mathbf{t}_{fi} = \begin{bmatrix} \omega_{fi} \\ \dot{\mathbf{c}} - d\dot{\psi}\mathbf{e}_i \end{bmatrix} \tag{20}$$

where

$$\omega_p = \dot{\psi} , \quad \omega_{fi} = \dot{\psi} + \dot{\varphi}_i . \tag{21}$$

The twists of the ball-wheels can be expressed, in turn, as the 5-dimensional vectors

$$\mathbf{t}_{bi} = \begin{bmatrix} \boldsymbol{\omega}_i \\ \dot{\mathbf{c}} - \dot{\psi}\mathbf{e}_i d \end{bmatrix} \tag{22}$$

where the 3-dimensional angular velocity vector $\boldsymbol{\omega}_i$ of the ball-wheels has been derived in the form

$$\boldsymbol{\omega}_i \equiv \begin{bmatrix} u_i \\ v_i \\ w_i \end{bmatrix} = \begin{bmatrix} \rho \mathbf{R}_i^{-1} \dot{\boldsymbol{\xi}}_i \\ \dot{\psi} + \dot{\varphi}_i \end{bmatrix} , \quad i = 1, 2, 3 \ . \tag{23}$$

The twists of the rollers R_l, R_m, and R_n are

$$\mathbf{t}_{li} = \begin{bmatrix} \boldsymbol{\omega}_{li} \\ \dot{\mathbf{c}}_{li} \end{bmatrix} , \quad \mathbf{t}_{mi} = \begin{bmatrix} \boldsymbol{\omega}_{mi} \\ \dot{\mathbf{c}}_{mi} \end{bmatrix} , \quad \mathbf{t}_{ni} = \begin{bmatrix} \boldsymbol{\omega}_{ni} \\ \dot{\mathbf{c}}_{ni} \end{bmatrix} \tag{24}$$

where

$$\begin{aligned} \dot{\mathbf{c}}_{ni} &= \dot{\mathbf{c}}_i + (R + r)(\dot{\psi} + \dot{\varphi}_i)\mathbf{l}_i \ , \\ \dot{\mathbf{c}}_{mi} &= \dot{\mathbf{c}}_i + (R + r)(\dot{\psi} + \dot{\varphi}_i)\mathbf{m}_i \ , \\ \dot{\mathbf{c}}_{ni} &= \dot{\mathbf{c}}_i + (R + r)(\dot{\psi} + \dot{\varphi}_i)\mathbf{n}_i \ , \end{aligned} \tag{25}$$

while the angular velocity vectors of the rollers are expressed in frames $\mathcal{R}_i$, defined along the principal axes of each roller, as

$$[\boldsymbol{\omega}_l]_i = \begin{bmatrix} \dot{\theta}_{li} \\ 0 \\ \dot{\psi} + \dot{\varphi}_i \end{bmatrix} , \quad [\boldsymbol{\omega}_m]_i = \begin{bmatrix} \dot{\theta}_{mi} \\ 0 \\ \dot{\psi} + \dot{\varphi}_i \end{bmatrix} ,$$

$$[\boldsymbol{\omega}_n]_i = \begin{bmatrix} \dot{\theta}_{ni} \\ 0 \\ \dot{\psi} + \dot{\varphi}_i \end{bmatrix} \tag{26}$$

where the first components of the above vectors are the roller axial angular velocities and the third components are the angular velocities of the rollers with respect to their central vertical axes.

We assume that each of the ball-carriers, ball-wheels, and rollers are identical, and we let H_p, H_f be the moments of inertia of the platform and the ball-carriers, correspondingly, with respect to their mass centers. Likewise, we let $\mathbf{J}_b$ and $\mathbf{J}_r$ be the 3×3 inertia matrices of the ball-wheels and of the rollers R_l, R_m, and R_n. Moreover, we let m_p, m_f, m_b, and m_r denote the masses of the corresponding bodies.

The kinetic energy of the unconstrained system is

$$T = T_p + T_f + T_b + T_r \tag{27}$$

where T_p, T_f, T_b, and T_r denote the kinetic energy of the platform, the ball-carriers, the balls, and the rollers, respectively, and can be expressed as:

$$\begin{aligned} T = \frac{1}{2}[m(\dot{x}^2 + \dot{y}^2) + (H_p + 3m_w d^2)\dot{\psi}^2 + H_w \sum_{i=1}^{3} (\dot{\psi} + \dot{\varphi}_i)^2 \\ + \left(\frac{2}{3}\rho^2 J_b + J_r\right) \sum_{i=1}^{3} \dot{\boldsymbol{\vartheta}}_i^T \dot{\boldsymbol{\vartheta}}_i] \end{aligned} \tag{28}$$

where

$$m \equiv m_p + 3m_w, \quad m_w \equiv m_f + m_b + 3m_r, \qquad (29)$$
$$H_w \equiv H_f + J_b + 3[J_h + m_r(R+r)^2] \ .$$

The kinetic energy of the constrained system can be written in the form

$$\tilde{T} = T_p + T_f + \tilde{T}_b + \tilde{T}_r = \frac{1}{2}[A\dot{\psi}^2 + B(\dot{x}^2 + \dot{y}^2) + H_w \sum_{i=1}^{3}(\dot{\psi} + \dot{\varphi}_i)^2] \quad (30)$$

where $\tilde{T}_b$ and $\tilde{T}_r$ denote the kinetic energy of the corresponding body after taking into account the nonholonomic constraints. Here we introduce the notation:

$$A \equiv H_p + 3\left[m_w + \left(\frac{J_b}{R^2} + \frac{3}{2}\frac{J_r}{r^2}\right)\right] d^2 \ ,$$
$$B \equiv m_p + 3\left[m_w + \left(\frac{J_b}{R^2} + \frac{3}{2}\frac{J_r}{r^2}\right)\right], \qquad (31)$$

with H_w and m_w defined in eq.(29).

4
The Mathematical Model

The Nonholonomic Term of the Governing Equations

We now derive the nonholonomic term of the governing equations as a product of the holonomy matrix $\mathbf{H}$ in eq.(18) and the 12-dimensional *unconstrained* momentum vector $\mathbf{p}$

$$\mathbf{p} \equiv \left[\begin{array}{cccc} \partial T/\partial\dot{\psi} & \partial T/\partial\dot{\mathbf{c}} & \partial T/\partial\dot{\boldsymbol{\xi}} & \partial T/\partial\dot{\boldsymbol{\varphi}} \end{array}\right]^T$$

in the form

$$\mathbf{H}\mathbf{p} = \left(\frac{J_b}{R^2} + \frac{3}{2}\frac{J_r}{r^2}\right)\mathbf{h} \ , \qquad (32)$$

with the five components of vector $\mathbf{h}$ defined as

$$h_1 \equiv d\sum_{i=1}^{3}[\dot{x}\sin(\psi+\delta_i) - \dot{y}\cos(\psi+\delta_i)](\dot{\psi}+\dot{\varphi}_i) \ ,$$
$$h_2 \equiv \sum_{i=1}^{3}[\dot{y} - \dot{\psi}d\sin(\psi+\delta_i)](\dot{\psi}+\dot{\varphi}_i) \ , \qquad (33)$$
$$h_3 \equiv \sum_{i=1}^{3}[\dot{x} - \dot{\psi}d\cos(\psi+\delta_i)](\dot{\psi}+\dot{\varphi}_i) \ ,$$
$$h_4 \equiv 0 \ , \quad h_5 \equiv 0 \ , \quad h_6 \equiv 0 \ .$$

Derivation of the Mathematical Model

General Case

We derive the governing equations of the nonholonomic system using the *constrained Lagrange equations*, as in [[9]]. We note first that the nonholonomic terms of the governing equations derived above, as well as the expression for the kinetic energy of the *constrained* system in eq.(30), happen to be independent of the choice of matrix $\mathbf{K}$, as defined in eq.(7). Hence, the left-hand side of the *constrained Lagrange equations* is also independent of $\mathbf{K}$. In fact, regardless of the choice of matrix $\mathbf{K}$, the mathematical model of this system takes the form

$$\tilde{\mathbf{I}}(\mathbf{s})\ddot{\mathbf{s}} + \boldsymbol{\chi}(\mathbf{s}, \dot{\mathbf{s}}) = \mathbf{f} \tag{34}$$

where $\boldsymbol{\chi}$ is the vector of Coriolis and centrifugal forces, discussed below, while $\mathbf{s}$ is the 6-dimensional vector of *independent* generalized coordinates of the system, with $\dot{\mathbf{s}} = \mathbf{u}$, namely,

$$\mathbf{s} \equiv [\ \psi \quad \mathbf{c}^T \quad \boldsymbol{\varphi}^T\ ]^T ,$$

and $\mathbf{f}$ is the 6-dimensional vector of *constrained* generalized forces of the system:

$$\mathbf{f} \equiv \begin{bmatrix} f_\psi(\mathbf{s}, \dot{\psi}) \\ \mathbf{f_c}(\mathbf{s}, \dot{\mathbf{c}}) \\ \mathbf{f}_\varphi(\mathbf{s}, \dot{\boldsymbol{\varphi}}) \end{bmatrix} = \mathbf{N}^T \boldsymbol{\phi} .$$

Moreover, $\boldsymbol{\phi}$ is the 12-dimensional vector of *unconstrained* generalized forces [[9]]. The 6×6 generalized inertia matrix $\tilde{\mathbf{I}}$ of the constrained system is

$$\tilde{\mathbf{I}} = \begin{bmatrix} A + 3H_w & \mathbf{0}_2^T & H_w \mathbf{1}_3^T \\ \mathbf{0}_2 & B\mathbf{1}_{2\times 2} & \mathbf{O}_{2\times 3} \\ H_w \mathbf{1}_3 & \mathbf{O}_{3\times 2} & H_w \mathbf{1}_{3\times 3} \end{bmatrix} \tag{35}$$

where constants H_w, A, and B have been defined in eqs.(29) and (31), respectively. The vector $\boldsymbol{\chi}$ of Coriolis and centrifugal forces of the governing equations of the constrained system comes from the nonholonomy terms, eq.(32), i.e.,

$$\boldsymbol{\chi}(\mathbf{s}, \dot{\mathbf{s}}) = \left(\frac{J_b}{R^2} + \frac{3}{2}\frac{J_r}{r^2}\right) \mathbf{h}(\mathbf{s}, \dot{\mathbf{s}}) . \tag{36}$$

As we can see from eqs.(32), (34), and (35), the contributions to the governing equation of the platform and ball-carriers are constant, while those of the ball-wheels and rollers are configuration dependent, and hence contribute to the Coriolis and centrifugal forces.

Moreover, the mathematical model of eq.(34) shows that the system at hand is a Chaplygin system [[8]]; that is, the dynamic equations and the kinematic constraint equations can be integrated separately. This means that one can run a simulation for the system using the governing equation (34); the "dependent" generalized velocity vectors $\dot{\boldsymbol{\xi}}_i, i = 1, 2, 3$, are then found from the constraint equations (13). This gives two components of vector $\dot{\boldsymbol{\theta}}_i$. The third component can be found using eq.(5). Vector $\boldsymbol{\theta}$, then, can be found by integration.

Actuation scheme

The system has a mobility of degree six and, hence, has to be driven by six actuators. This can be done in a few ways, e.g., by actuating *i*) six rollers or *ii*) three rollers and three ball-carriers. However, it turns out that only the case *ii*) is feasible, as we now show. From eq.(2), we have

$$\dot{\mathbf{c}} = \frac{1}{3}\sum_{i=1}^{3}\dot{\mathbf{c}}_i \quad \text{and} \quad \dot{\psi} = -\frac{1}{3d}\sum_{i=1}^{3}\mathbf{e}_i^T\dot{\mathbf{c}}_i \ . \tag{37}$$

Substituting eq.(2) into eq.(12), we obtain

$$\dot{\mathbf{c}}_i = r\mathbf{E}^T\mathbf{R}_i^{-1}\dot{\boldsymbol{\xi}}_i \ ,$$

and hence, after substituting the above expression into eqs.(37),

$$\dot{\mathbf{c}} = \frac{1}{3}r\mathbf{E}^T\sum_{i=1}^{3}\mathbf{R}_i^{-1}\dot{\boldsymbol{\xi}}_i, \quad \dot{\psi} = -\frac{r}{3d}\sum_{i=1}^{3}\mathbf{e}_i^T\mathbf{E}^T\mathbf{R}_i^{-1}\dot{\boldsymbol{\xi}}_i \ .$$

Since the components of the 6-dimensional vector $\dot{\boldsymbol{\xi}}$, defined in eqs.(4) and (6), are constrained by the three above equations, only three of these components are independent and, hence, can be actuated independently. Therefore, one actuator can be connected to each of three rollers, one roller per ball, and three more actuators should be introduced to control the orientation of the ball-carriers with respect to the platform.

If we denote by $\mathbf{v}_r$ the 3-dimensional vector of the motor-shaft rates connected to the three rollers, one per ball-wheel, and by $\mathbf{v}_b$ the 3-dimensional vector of the motor-shaft rates connected to the three ball-carriers, then we can write the relations

$$\mathbf{v}_r = \boldsymbol{\Lambda}_r\dot{\boldsymbol{\xi}} \ , \quad \mathbf{v}_b = \lambda_b\dot{\boldsymbol{\varphi}}, \tag{38}$$

or

$$\mathbf{v} \equiv \begin{bmatrix} \mathbf{v}_r \\ \mathbf{v}_b \end{bmatrix} = \begin{bmatrix} \boldsymbol{\Lambda}_r & \mathbf{O}_{3\times 3} \\ \mathbf{O}_{3\times 6} & \lambda_b\mathbf{1}_{3\times 3} \end{bmatrix} \begin{bmatrix} \dot{\boldsymbol{\xi}} \\ \dot{\boldsymbol{\varphi}} \end{bmatrix} \tag{39}$$

where the 3×6 matrix $\boldsymbol{\Lambda}_r$ is given by

$$\boldsymbol{\Lambda}_r \equiv \lambda_r \begin{bmatrix} (\boldsymbol{\kappa}_j^T)_1 & \mathbf{0}_2^T & \mathbf{0}_2^T \\ \mathbf{0}_2^T & (\boldsymbol{\kappa}_j^T)_2 & \mathbf{0}_2^T \\ \mathbf{0}_2^T & \mathbf{0}_2^T & (\boldsymbol{\kappa}_j^T)_3 \end{bmatrix}, \quad j = 1, 2,$$

$$\boldsymbol{\kappa}_1 \equiv \begin{bmatrix} 1 \\ 0 \end{bmatrix}, \quad \boldsymbol{\kappa}_2 \equiv \begin{bmatrix} 0 \\ 1 \end{bmatrix}$$

with $(\boldsymbol{\kappa}_j^T)_i$ $i = 1, 2, 3$, indicating the wheel number. Next, we group the torques applied to the rollers into a 6-dimensional vector $\mathbf{n}_r$, which is obtained as

$$\mathbf{n}_r = \boldsymbol{\Lambda}_r^T(\boldsymbol{\tau}_r - \mathbf{J}_1\dot{\mathbf{v}}_r) \ , \tag{40}$$

and the torques applied to the ball-carriers are grouped into a 3-dimensional vector $\mathbf{n}_b$, given by

$$\mathbf{n}_b = \lambda_b(\boldsymbol{\tau}_b - \mathbf{J}_2\dot{\mathbf{v}}_b)$$

where $\mathbf{J}_1$ and $\mathbf{J}_2$ are the 3×3 generalized inertia matrices for the actuator shafts and $\boldsymbol{\tau}_r, \boldsymbol{\tau}_b$ are vectors of torques exerted by the actuators. Therefore, we can express the 9-dimensional generalized torque vector in the form

$$\mathbf{n} = \begin{bmatrix} \mathbf{n}_r \\ \mathbf{n}_b \end{bmatrix} = \begin{bmatrix} \boldsymbol{\Lambda}_r^T & \mathbf{O}_{6\times 3} \\ \mathbf{O}_{3\times 3} & \lambda_b \mathbf{1}_{3\times 3} \end{bmatrix} (\boldsymbol{\tau} - \mathbf{J}_m\dot{\mathbf{v}})$$

where

$$\boldsymbol{\tau} \equiv \begin{bmatrix} \boldsymbol{\tau}_r \\ \boldsymbol{\tau}_b \end{bmatrix}, \quad \mathbf{J}_m \equiv \begin{bmatrix} \mathbf{J}_1 & \mathbf{O}_{3\times 3} \\ \mathbf{O}_{3\times 3} & \mathbf{J}_2 \end{bmatrix}, \quad \dot{\mathbf{v}} \equiv \begin{bmatrix} \dot{\mathbf{v}}_r \\ \dot{\mathbf{v}}_b \end{bmatrix} .$$

The 12-dimensional vector of *unconstrained* generalized forces in this case is

$$\boldsymbol{\phi} = \begin{bmatrix} \mathbf{0}_3 \\ \boldsymbol{\Lambda}_r^T(\boldsymbol{\tau}_r - \mathbf{J}_1\dot{\mathbf{v}}_r) \\ \lambda_b(\boldsymbol{\tau}_b - \mathbf{J}_2\dot{\mathbf{v}}_b) \end{bmatrix} ,$$

the 6-dimensional vector of *constrained* generalized forces being, in turn,

$$\mathbf{f} \equiv \mathbf{N}^T\boldsymbol{\phi} = \begin{bmatrix} \boldsymbol{\Gamma}_1^T & \mathbf{O}_{3\times 3} \\ \mathbf{O}_{3\times 3} & \lambda_b \mathbf{1}_{3\times 3} \end{bmatrix} (\boldsymbol{\tau} - \mathbf{J}_m\dot{\mathbf{v}}) = \boldsymbol{\Gamma}^T(\boldsymbol{\tau} - \mathbf{J}_m\dot{\mathbf{v}}) \tag{41}$$

where

$$\boldsymbol{\Gamma}_1 \equiv \boldsymbol{\Lambda}_r\boldsymbol{\Upsilon}', \ \boldsymbol{\Upsilon}' \equiv \frac{1}{r}\begin{bmatrix} \boldsymbol{\alpha}d & -\mathbf{S} \end{bmatrix}, \ \boldsymbol{\Gamma} \equiv \begin{bmatrix} \boldsymbol{\Gamma}_1 & \mathbf{O}_{3\times 3} \\ \mathbf{O}_{3\times 3} & \lambda_b \mathbf{1}_{3\times 3} \end{bmatrix}. \tag{42}$$

Furthermore, from eqs.(39), using eqs.(15) and (42), we derive

$$\mathbf{v} \equiv \begin{bmatrix} \mathbf{v}_r \\ \mathbf{v}_b \end{bmatrix} = \begin{bmatrix} \boldsymbol{\Gamma}_1 & \mathbf{O}_{3\times 3} \\ \mathbf{O}_{3\times 3} & \lambda_f \mathbf{1}_{3\times 3} \end{bmatrix} \dot{\mathbf{s}} = \boldsymbol{\Gamma}\dot{\mathbf{s}} . \tag{43}$$

Hence, we have

$$\dot{\mathbf{v}} \equiv \begin{bmatrix} \dot{\mathbf{v}}_r \\ \dot{\mathbf{v}}_b \end{bmatrix} = \boldsymbol{\Gamma}\ddot{\mathbf{s}} + \dot{\boldsymbol{\Gamma}}\dot{\mathbf{s}} \tag{44}$$

where

$$\dot{\boldsymbol{\Gamma}} = \begin{bmatrix} \dot{\boldsymbol{\Gamma}}_1 & \mathbf{O}_{3\times 3} \\ \mathbf{O}_{3\times 3} & \mathbf{O}_{3\times 3} \end{bmatrix} \quad \text{and} \quad \dot{\boldsymbol{\Gamma}}_1 = \boldsymbol{\Lambda}_r\dot{\boldsymbol{\Upsilon}}_1 = \boldsymbol{\Lambda}_r\frac{1}{r}\begin{bmatrix} \dot{\boldsymbol{\alpha}}d & -\dot{\mathbf{S}} \end{bmatrix} .$$

Therefore, the governing eq.(34) can be written in the form

$$\left(\tilde{\mathbf{I}} + \boldsymbol{\Gamma}^T\mathbf{J}_m\boldsymbol{\Gamma}\right)\ddot{\mathbf{s}} + \boldsymbol{\Gamma}^T\mathbf{J}_m\dot{\boldsymbol{\Gamma}}\dot{\mathbf{s}} + \boldsymbol{\chi}(\mathbf{s}, \dot{\mathbf{s}}) = \boldsymbol{\Gamma}^T\boldsymbol{\tau} , \tag{45}$$

with

$$\boldsymbol{\tau} = \begin{bmatrix} \boldsymbol{\tau}_r \\ \boldsymbol{\tau}_b \end{bmatrix} = \begin{bmatrix} k_r\boldsymbol{\iota}_r \\ k_b\boldsymbol{\iota}_b \end{bmatrix}$$

where k_r, k_b are the motor torque constants and $\boldsymbol{\iota}_r, \boldsymbol{\iota}_b$ are the motor currents.

5 Implementation of the Simplifying Constraints

As can be seen from eqs.(33) and (36), if $\omega_i \equiv \dot{\psi} + \dot{\varphi}_i \equiv 0$, for $i = 1, 2, 3$, then the nonholonomy term $\boldsymbol{\chi}$ in the governing equation (45) vanishes. Hence, to simplify the control of the system, we impose the constraints $\omega_i = 0$ on the ball-carriers that prevent them from changing their orientation with respect to an inertial frame. In practice, this can be done by connecting the ball-carriers by belt-pulley transmissions to a central platform (CP), as shown in Fig. 4, while maintaining the constant orientation of this platform with respect to an inertial frame. The centroid of the CP

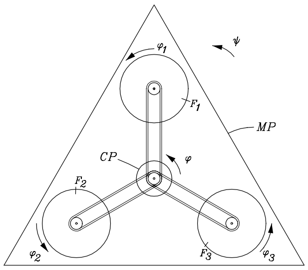

Figure 4: Connection the central platform (CP) with the ball-carriers

coincides with that of the main platform (MP), both being coupled by a revolute joint whose axis is perpendicular to the plane of motion. One way to maintain the constant orientation of the CP with respect to an inertial frame is by introducing a planetary gear train (PGT) with two degrees of freedom, similar to the one described in [[2]] for the Chinese south-pointing chariot. To implement this solution, we should couple the MP by a revolute joint to an axle with two identical small wheels. These wheels can rotate freely with respect to the axis of this axle. In [[2]], a few design examples of this PGT are described for two possible cases: *i*) the carrier of the PGT is adjacent to the CP, while the sun gears are adjacent to the left and right wheels of the axle; and *ii*) one sun gear is adjacent to the CP, while another sun gear and carrier are adjacent to the two wheels.

Another implementation consists of controlling electronically the orientation of the CP and, therefore, of the ball-carriers, connected to the CP by belts. The objective is to keep the angular velocity of the CP equal to zero under any motion of the MP. To this end, the angular velocity of the CP should be measured. This can be achieved, e.g., by coupling two axles, with two small wheels each, to the CP by revolute joints and placing tachometers on each wheel. The details of this array are given in [[10]].

The System in Holonomic Mode

The constraints that prevent the ball-carriers from changing their orientation with respect to an inertial frame are $\omega_i = 0$ or $\dot{\varphi}_i = -\dot{\psi}$, for $i = 1, 2, 3$. By this, we compensate the rotation of the platform ψ with a counter-rotation $-\psi$ of the ball-carriers with respect to the platform, i.e., we impose the geometric constraints $\varphi_1 = \varphi_2 = \varphi_3 = -\psi$. If $\dot{\psi} + \dot{\varphi}_i = 0$, for $i = 1, 2, 3$, then all three ball-carriers undergo a pure translation in the inertial frame, the term $\boldsymbol{\chi}(\mathbf{s}, \dot{\mathbf{s}})$ in the left-hand side of eq.(45) vanishes, and the system becomes holonomic with three dof, as shown in [[9]]. Therefore, a three-dimensional vector of generalized coordinates can be chosen as

$$\mathbf{q} = \begin{bmatrix} \psi & x & y \end{bmatrix}^T .$$

The constraint equation (12) for this simplified system is integrable because the 2×2 matrices $\mathbf{R}_i$ are constant, i.e.,

$$\mathbf{R}_i = \mathbf{K} \begin{bmatrix} -\cos\delta_l & -\sin\delta_l \\ -\cos\delta_m & -\sin\delta_m \\ -\cos\delta_n & -\sin\delta_n \end{bmatrix} .$$

Integrating eq.(12) and taking into account the appropriate initial conditions, we derive the corresponding geometrical constraint in the form:

$$\mathbf{c} + r\mathbf{E}\mathbf{R}^{-1}\boldsymbol{\xi}_i + \mathbf{f}_i d = \boldsymbol{\beta}$$

where $\boldsymbol{\beta}$ is a constant of integration:

$$\boldsymbol{\beta} = \mathbf{c}_O + r\mathbf{E}\mathbf{R}^{-1}[\boldsymbol{\xi}_i]_0 + [\mathbf{f}_i]_0 d .$$

The generalized inertia matrix $\mathbf{I}$ for this holonomic system is also a 3×3 constant matrix, namely,

$$\mathbf{I} = \begin{bmatrix} A & \mathbf{0}_2^T \\ \mathbf{0}_2 & B\mathbf{1}_{2\times 2} \end{bmatrix} .$$

The governing equations thus reduce to

$$\mathbf{I}\ddot{\mathbf{q}} = \mathbf{f}$$

where $\mathbf{f}$ is the vector of generalized forces:

$$\mathbf{f} \equiv [\ f_\psi \quad f_x \quad f_y\ ]^T .$$

Since the system has three dof, it has to be driven by three actuators. This can be done by three DC motors driving three rollers, one per ball-wheel. If we denote by $\mathbf{v}$ the vector of the motor-shaft rates, then we can write the relation

$$\mathbf{v} = \boldsymbol{\Lambda}\dot{\boldsymbol{\xi}} .$$

Following the same procedure as above, we derive $\mathbf{n}_r$ as in eq.(40). Then, the vector of generalized forces is

$$\mathbf{f} = \frac{1}{r} \begin{bmatrix} \boldsymbol{\alpha}^T \boldsymbol{\Lambda}^T (\boldsymbol{\tau}_m - \mathbf{J}_m \dot{\mathbf{v}}) d \\ -\mathbf{S}^T \boldsymbol{\Lambda}^T (\boldsymbol{\tau}_m - \mathbf{J}_m \dot{\mathbf{v}}) \end{bmatrix} = \boldsymbol{\Gamma}_1^T (\boldsymbol{\tau}_m - \mathbf{J}_m \dot{\mathbf{v}})$$

where $\mathbf{\Gamma}_1$ is defined in eq.(42). Since in this case matrix $\mathbf{S}$ is constant and vector $\boldsymbol{\alpha}$ of eqs.(14) is a function of ψ only, we have

$$\dot{\mathbf{\Gamma}}_1\dot{\mathbf{q}} = \mathbf{\Lambda}\begin{bmatrix} \boldsymbol{\alpha}' & \mathbf{O}_{6\times 2} \end{bmatrix}\dot{\mathbf{q}}(-\dot{\psi})d = -\mathbf{\Lambda}\boldsymbol{\alpha}'\dot{\psi}^2 d\ .$$

Therefore, the governing equation for the simplified model in holonomic mode takes the form:

$$(\mathbf{I} + \mathbf{\Gamma}_1^T\mathbf{J}_m\mathbf{\Gamma}_1)\ddot{\mathbf{q}} - \mathbf{\Gamma}_1^T\mathbf{J}_m\mathbf{\Lambda}\boldsymbol{\alpha}'\dot{\psi}^2 d = \mathbf{\Gamma}_1^T K_r\boldsymbol{\iota}\ .$$

The Simplified System in Nonholonomic Mode

If in some instants during the motion, $\dot{\psi}+\dot{\varphi}_i$ differs from zero, then one can conclude that the system has switched from holonomic to nonholonomic mode. By means of the array shown in Fig. 4, and since $\varphi_1 = \varphi_2 = \varphi_3 = \varphi_p$, the degree of mobility of the system is reduced in nonholonomic mode to four. Therefore, the independent velocity vector $\mathbf{u}$ is now four dimensional, namely,

$$\mathbf{u} \equiv \dot{\mathbf{s}} = \begin{bmatrix} \dot{\psi} & \dot{\mathbf{c}} & \dot{\varphi}_p \end{bmatrix}^T \tag{46}$$

and, since for this scheme

$$\tilde{T} = \frac{1}{2}[A\dot{\psi}^2 + B(\dot{x}^2 + \dot{y}^2) + 3H_w(\dot{\psi} + \dot{\varphi}_p)^2]\ , \tag{47}$$

the mass matrix $\tilde{\mathbf{I}}$ in eq.(34) is of 4×4, i.e.,

$$\tilde{\mathbf{I}} = \begin{bmatrix} A + 3H_w & \mathbf{0}_2^T & 3H_w \\ \mathbf{0}_2 & B\mathbf{1}_{2\times 2} & \mathbf{0}_2 \\ 3H_w & \mathbf{0}_2^T & 3H_w \end{bmatrix}\ . \tag{48}$$

Vector $\mathbf{h}$ of eq.(32) is also four dimensional. Moreover, since

$$\sum_{i=1}^{3}\sin(\psi + \delta_i) = 0\ , \quad \sum_{i=1}^{3}\cos(\psi + \delta_i) = 0\ ,$$

we have

$$h_1 = 0\ , \quad h_2 = 3(\dot{\psi} + \dot{\varphi}_p)\dot{y}\ , \quad h_3 = 3(\dot{\psi} + \dot{\varphi}_p)\dot{x}\ , \quad h_4 \equiv 0\ .$$

Vector $\mathbf{v}$ of eq.(39) is also four dimensional, namely,

$$\mathbf{v} = \begin{bmatrix} \mathbf{v}_r & v_b \end{bmatrix}^T\ ,$$

and J_2 and τ_b are scalars. Therefore, the vector of *constrained* general forces $\mathbf{f}$ is also four dimensional:

$$\mathbf{f} = \mathbf{\Gamma}^T(\boldsymbol{\tau} - \mathbf{J}_m\dot{\mathbf{v}})\ ,$$

with

$$\mathbf{\Gamma} = \begin{bmatrix} \mathbf{\Gamma}_1^T & \mathbf{0}_3 \\ \mathbf{0}_3^T & \lambda_b \end{bmatrix}\ , \quad \mathbf{J}_m = \begin{bmatrix} \mathbf{J}_1 & \mathbf{0}_3 \\ \mathbf{0}_3^T & J_2 \end{bmatrix}$$

being 4×4 matrices. The governing equation (45) for the simplified system in nonholonomic mode can therefore be written in the form:

$$\left(\tilde{\mathbf{I}} + \mathbf{\Gamma}^T\mathbf{J}_m\mathbf{\Gamma}\right)\ddot{\mathbf{s}} + \mathbf{\Gamma}^T\mathbf{J}_m\dot{\mathbf{\Gamma}}\dot{\mathbf{s}} + \left(\frac{J_b}{R^2} + \frac{3}{2}\frac{J_r}{r^2}\right)\mathbf{h} = \mathbf{\Gamma}^T\boldsymbol{\tau}\ . \tag{49}$$

6 Simulation

We have performed independent numerical simulations of eq.(49) using the multi-body system integrator library MBSSIM [[14]] and Matlab's Simulink toolbox [[15]]. The use of these simulation packages allows us to have a wide selection of integration methods, as well as several linear algebra routines to invert the generalized inertia matrix in eq.(49).

One of the goals of our simulation is to study the relative efficiency of simulating the system in holonomic versus nonholonomic mode. We are also interested in investigating the smoothness of the motion in the two modes. Since we have yet to carefully study the stable control of such a system with regard to task execution or selection matrix for actuation (7), we simply use a constant input $\boldsymbol{\tau}$, the selection matrices

$$\mathbf{K}_1 = \begin{bmatrix} 1 & 0 & 0 \\ 0 & 1 & 0 \end{bmatrix}, \quad \mathbf{K}_2 = \begin{bmatrix} 0 & 1 & 0 \\ 0 & 0 & 1 \end{bmatrix}, \quad \mathbf{K}_3 = \begin{bmatrix} 1 & 0 & 0 \\ 0 & 0 & 1 \end{bmatrix},$$

corresponding to wheels 1, 2, and 3, respectively, and $\boldsymbol{\kappa} = [\ 1 \quad 0\ ]^T$. Below, we report some results for one such simulation. The system parameters used are

$$\begin{aligned} d &= 0.5 \text{ m}, & r &= 0.125 \text{ m}, & R &= 0.5 \text{ m}, \\ J_b &= 6 \text{ kg m}^2, & J_r &= 2 \text{ kg m}^2, & \lambda_b &= \lambda_r = 80, \\ H_w &= 1 \text{ kg m}^2, & A &= 1 \text{ kg m}^2, & B &= 2 \text{ kg}, \end{aligned}$$

with

$$J_1 = 2\, \mathbf{1}_{3\times 3} \text{ kg m}^2, \quad \text{and } J_2 = 2 \text{ kg m}^2.$$

In Figs.5 and 6, we show, respectively, the trajectory of the centroid C

Figure 5: Cartesian trajectory of centroid C and angular velocity of the main platform in holonomic (—) vs. nonholonomic (- - -) mode.

of the robot and the velocities $\dot{\psi}$, $\dot{x}$, and $\dot{y}$ of the platform orientation ψ and the position coordinates x and y of the centroid C of the robot.

Figure 6: x- and y-components of robot mass-center velocity in holonomic (—) vs. non-holonomic mode (- - -).

We expect that the motion of C near rest ($\dot{\mathbf{q}} = \mathbf{0}$) under the given actuation scheme and constant input $\boldsymbol{\tau}$ should be approximately rectilinear. We see that this is indeed the case for the motion in holonomic mode. On the other hand, the motion in nonholonomic mode departs from straight-line motion much more quickly.

Execution statistics for runs of 50 seconds are shown in Tables 1 and 2. For a given tolerance, we display the relative CPU time taken in executing the run, the status flag, the number of integration steps attempted, broken down into the number accepted and the number rejected, the number of times the generalized inertia matrix was evaluated (and inverted), and the number of times the right-hand side was evaluated.

As we might anticipate, simulation of the holonomic system requires less CPU time than simulation of the corresponding nonholonomic system because the holonomic system has fewer terms and is of smaller dimension. However, these are not the only relevant considerations. We also note that the number of integration steps required is much less for the same tolerance and simulation time in the case of the *simpler* dynamics produced in holonomic mode. Most notably, the computational work done in performing the simulations of the system in holonomic mode do not change as the tolerance is decreased. Simulation of more complex system generally necessitates more computational expense than simulation of simpler system mainly due to the smaller steps that the integrator is forced to take. Moreover, there is a smaller chance of producing spurious results when simulating motion in holonomic mode. In the course of our numerical experiments, we have noticed incorrect results produced by the simulation of motion in nonholonomic mode as a function of the specified tolerance and integration scheme (e.g., Runge-Kutta versus Adams-Bashforth). The combination of these factors implies that the system in holonomic mode can be simulated much more efficiently and reliably than in nonholonomic mode.

$-\log$ (TOL)	CPU	OK	STPS	ACPT	RJCT	NMAT	NRHS
2.0	0.1	1	13	13	0	31	32
4.0	0.1	1	13	13	0	31	32
6.0	0.1	1	13	13	0	31	32
8.0	0.1	1	13	13	0	31	32
10.0	0.1	1	14	14	0	33	34

Table 1: Execution statistics for motion in holonomic mode.

$-\log$ (TOL)	CPU	OK	STPS	ACPT	RJCT	NMAT	NRHS
2.0	0.8	1	279	141	138	3430	3431
4.0	1.1	1	370	250	120	4627	4628
6.0	1.6	1	557	408	149	6926	6927
8.0	2.1	1	777	592	185	9593	9594
10.0	3.2	1	1234	950	284	15062	15063

Table 2: Execution statistics for motion in nonholonomic mode.

7
Conclusions

The mathematical model developed for the robot under study can be identified as a Chaplygin system. This implies that the system of dynamic equations is decoupled from the system of kinematic constraint equations. Therefore, these equations can be integrated separately. Thus, instead of integrating a system of n second-order ODEs, we can integrate separately a system of $n-p$ second-order ODEs and a system of p first-order ODEs.

To actuate the system, one actuator is connected to one roller of each wheel, with three more actuators controlling the orientation of the ball-carriers with respect to the platform.

As a result of studying the mathematical model of this system by using the *holonomy matrix* [[9]], conditions are found under which the system can be rendered holonomic. Therefore, to simplify the control of the system, we impose constraints on the ball-carriers that prevent them from changing their orientation with respect to an inertial frame, thereby maintaining holonomicity.

We are currently investigating the controller design based on the dynamics analysis reported here, along with implementation of the trajectory controller.

Acknowledgements

This work was made possible by the Natural Sciences and Engineering Research Council (NSERC) of Canada. The second author was also partially supported under a CRM-ISM (Centre de Recherches Mathématiques-Institut des Sciences Mathématiques) Postdoctoral Fellowship.

References

[Sim, 1995] (1995). *Simulink. Dynamic System Simulation Software.* The Math Works Inc., Natick, Mass.

[Fujisawa et al., 1998] Fujisawa, S., Umemoto, T., Shidama, Y., Ohkubo, K., Yoshida, T., and Yamaura, H. (1998). Development of an omnidirectional spherical robot and its moving properties. In *Proceedings of the 29th International Symposium on Robotics (ISR98). Advanced Robotics: Beyond 2000*, pages 236–239.

[Hsieh et al., 1996] Hsieh, L.-C., Liu, J.-Y., and Hsu, M.-H. (1996). Systematic method for the synthesis of south pointing chariot with planetary gear trains. *Transactions of Canadian Society for Mechanical Engineering*, 20(4):421–435.

[Koshiyama and Yamafuji, 1993] Koshiyama, A. and Yamafuji, K. (1993). Design and control of an all-direction steering type mobile robot. *The International Journal of Robotics Research*, 12(5):411–419.

[Luo et al., 1998] Luo, Z.-H., Machida, K., and Funaki, M. (1998). Design and control of a cartesian nonholonomic robot. *Journal of Robotic Systems*, 15(2):85–95.

[Mascaro et al., 1997] Mascaro, S., Spano, J., and Asada, H. H. (1997). A reconfigurable holonomic omnidirectional mobile bed with unified seating (rhombus) for bedridden patients. In *Proceedings of the 1997 IEEE International Conference on Robotics and Automation*, volume 2, pages 1277–1282. IEEE.

[Muir and Neuman, 1987] Muir, P. F. and Neuman, C. P. (1987). Kinematic modeling for feedback control of an omnidirectional wheeled mobile robot. In *International Conference on Robotics and Automation*, pages 1772–1778, New York. IEEE.

[Muir and Neuman, 1988] Muir, P. F. and Neuman, C. P. (1988). Dynamic modeling of multibody robotic mechanisms: Incorporating closed-chains, friction, higher-pair joints, and unactuated and unsensed joints. In *International Conference on Robotics and Automation*, volume 3, pages 1546–1551, Philadelphia. IEEE.

[Neimark and Fufaev, 1972] Neimark, J. and Fufaev, N. (1972). *Dynamics of Nonholonomic Systems.* American Mathematical Society, Providence, Rhode Island. Translations of Mathematical Monographs 33 (originally in Russian, 1967).

[Ostrovskaya and Angeles, 1998a] Ostrovskaya, S. and Angeles, J. (1998a). The kinematic analysis of the velocity sensor of a mobile robot with three ball-wheels. Technical report, CIM, McGill, Montreal.

[Ostrovskaya and Angeles, 1998b] Ostrovskaya, S. and Angeles, J. (1998b). Nonholonomic systems revisited within the framework of analytical mechanics. *Applied Mechanics Reviews*, pages 415–433.

[Paula, 1997] Paula, G. (1997). Cobots for the assembly line. *Mechanical Engineering*, 119(10):82–84.

[Pin and Killough, 1994] Pin, F. and Killough, S. (1994). A new family of omnidirectional and holonomic wheeled platforms for mobile robots. In *IEEE Transactions on Robotics and Automation*, volume 10, pages 480–489.

[Saha et al., 1995] Saha, S., Angeles, J., and Darcovich, J. (1995). The design of kinematically isotropic rolling robots with omnidirectional wheels. *Mechanism and Machine Theory*, 30(8):1127–1137.

[Tang et al., 1996] Tang, J., Watanabe, K., and Shiraishi, Y. (1996). Design and traveling experiment of an omnidirectional holonomic mobile robot. In *Proceedings of the 1996 IEEE/RSJ International Conference on Intelligent Robots and Systems. Robotic Intelligence Interacting with Dynamic Worlds. IROS'96*, volume 1, pages 66–73, Piscataway, NY, USA.

[von Schwerin and Winckler, 1994] von Schwerin, R. and Winckler, M. (1994). A guide to the integrator library MBSSIM, Version 1.00. Technical report, Interdisziplinäres Zentrum für Wissenschaftliches Rechnen, Universität Heidelberg.

[Wada and Mori, 1996] Wada, M. and Mori, S. (1996). Holonomic and omnidirectional vehicle with conventional tires. In *Proceedings of the 1996 International Conference on Robotics and Automation*, pages 3671–3676, Minneapolis, Minnesota. IEEE.

[Wada et al., 1995] Wada, M., Tominaga, Y., and Mori, S. (1995). Omnidirectional holonomic mobile robot using nonholonomic wheels. In *Proceedings of the 1995 IEEE/RSJ International Conference on Intelligent Robot and Systems. Human Robot Interaction and Cooperative Robots. IROS'95*, volume 3, pages 446–453, Los Alamita, California.

[West and Asada, 1992] West, M. and Asada, H. (1992). Design of a holonomic omnidirectional vehicle. In *IEEE Int. Conf. on Robotics and Automation*, pages 97–103, Nice, France. IEEE.

[West and Asada, 1995a] West, M. and Asada, H. (1995a). Design and control of ball wheel omnidirectional vehicles. In *Proceedings of 1995 IEEE International Conference on Robotics and Automation*, volume 2, pages 1931–1938, Nagoya, Japan. Japan Soc. Mech. Eng. IEEE Robotics and Autom.

[West and Asada, 1995b] West, M. and Asada, H. (1995b). Method for designing ball wheels for omnidirectional vehicles. In *Proceedings of the 1995 ASME Design Engineering Technical Conferences*, volume 82, pages 803–809, Cambridge, MA. Massachusetts Inst of Technology.

[West and Asada, 1997] West, M. and Asada, H. (1997). Design of ball wheel mechanisms for omnidirectional vehicles with full mobility and invariant kinematics. *ASME Journal of Mechanical Design*, 119(2):153–161.